

# HOMRS: High Order Metamorphic Relations Selector for Deep Neural Networks

FLORIAN TAMBON, Polytechnique Montréal, Canada

GIULIO ANTONIOL, Polytechnique Montréal, Canada

FOUTSE KHOMH, Polytechnique Montréal, Canada

Deep Neural Networks (DNN) applications are increasingly becoming a part of our everyday life, from medical applications to autonomous cars. Traditional validation of DNN relies on accuracy measures, however, the existence of adversarial examples has highlighted the limitations of these accuracy measures, raising concerns especially when DNN are integrated into safety-critical systems. In this paper, we present HOMRS, an approach to boost metamorphic testing by automatically building a small optimized set of high order metamorphic relations from an initial set of elementary metamorphic relations. HOMRS' backbone is a multi-objective search; it exploits ideas drawn from traditional systems testing such as code coverage, test case, and path diversity. We applied HOMRS to LeNet5 DNN with MNIST dataset and we report evidence that it builds a small but effective set of high order transformations achieving a 95% kill ratio. Five raters manually labelled a pool of images before and after high order transformation; Fleiss' Kappa and statistical tests confirmed that they are metamorphic properties. HOMRS built-in relations are also effective to confront adversarial or out-of-distribution examples; HOMRS detected 92% of randomly sampled out of distribution images. HOMRS transformations are also suitable for on-line real-time use.

CCS Concepts: • **Computing methodologies** → **Neural networks**.

Additional Key Words and Phrases: testing, metamorphic testing, neural network, out-of-distribution, adversarial examples, optimization

## 1 INTRODUCTION

Machine Learning (ML) applications (MLAs) and ML components such as Deep Neural Networks (DNN), like any software program, need to be tested. This is especially true when DNN are used in safety-critical systems such as autonomous driving or aerospace applications, where a failure can lead to disastrous consequences. Traditional software development uses a variety of verification and validation techniques to ensure characteristics such as reliability, dependability, or safety. For example, critical avionic applications must comply with certification standards such as the DO-178C that requires the adoption of specific practices and processes (*e.g.*, traceability), as well as precise testing criteria (*e.g.*, MCDC).

In contrast, MLAs and DNN correctness have traditionally been quantified through accuracy measures (*e.g.*, false positive rate, false negative rate, the AUC area, etc). The assumption was that a high accuracy system will perform as expected. However, the proof of the existence of Adversarial [5] or Out-Of-Distribution [1] (OOD) examples that made systems with high accuracy fail, have raised serious concerns. Unfortunately, DNN and MLAs are especially challenging to test, they, oftentimes, belong to the category of programs computing an unknown answer; since the answer is unknown, they lack a mechanism to determine the correctness of the output, *i.e.*, an oracle [37].

Metamorphic Testing (MT) [7] is a “pseudo-oracle” technique originally designed to alleviate the oracle problem. It has been applied both in traditional software testing [11] as well as in ML [39]; it has been adapted to test data generation [36]; and to detect Adversarial Examples (AE) attacks [26]. Metamorphic Relations (MRs) are the cornerstone of MT. A MR is a necessary property of an

intended software functionality. MRs hold true across executions. For example, a mug in a picture, remains a mug if we change the contrast, colour, or we blur the picture. We may not know the content of a picture, but, if a DNN trained to detect mugs, produces two different classifications on the original picture and on the MR transformed picture, then we know that something went wrong. MRs are generally defined by researchers and through catalogs of existing MRs [39]. Still, it is hard to know what the most effective MR will be and the notion of “good” relation is an ambiguous issue. Yet some rules of thumb were empirically established [33], emphasizing principally on the diversity of the relations used. Recently, several approaches have been proposed to automatically identify MRs, *e.g.*, [8, 41, 42]. However, these approaches are either limited to specific types of MRs (*e.g.*, polynomial MRs), and/or require testers to possess solid knowledge about the problem domain (*e.g.*, being able to make category-choice specification for a given problem). Moreover, those approaches weren’t applied to DNN, thus not taking into account their specificity and how it can impact MRs choice. To the best of our knowledge, no efficient approach exist for the automatic identification of high order MRs for DNN.

In this paper we present HOMRS, a High Order Metamorphic Relation Selector for the generation of an optimized set of High order Metamorphic Relations (HMRs) for ML/DNN testing. A High Order Metamorphic Relation (HMR) is defined via relation composition, more precisely, HOMRS represents HMRs as function composition, over a set of pre-existing elementary MRs. Optimized HMRs could then be used in an online fashion to test DNN in real time, similarly to what is done for traditional software [9, 28]. HOMRS strives to obtain an optimized set of HMRs outperforming the elementary MRs, in term of MT effectiveness, and execution time (*i.e.*, applying the HMRs should be faster or comparable to applying each and every elementary MRs).

HOMRS works off-line; it uses a test and train set. The train set is used for standard training of DNN. The test set is split into multiple smaller batches. Each batch is used to combine MRs into HMR via meta-heuristic multi-objective optimization generating multiple HMRs sets. HOMRS uses the NSGA-II method [10]. Finally, the most similar and most effective HMRs across batches are used to synthesize a new set, benchmarked on the whole test set. In a way, HOMRS, is similar to techniques such as DeepEvolution [3], with an opposite philosophy; *i.e.*, rather than using a lot of relations to mutate a small number of test data as it was done previously, we select a small optimized set of relations that are relevant for the whole test dataset, in order to improve the generalization power and hence relevance.

We applied HOMRS to DNN, more precisely, to LeNet5 [22] DNN using the MNIST dataset [23], and answered the following research questions:

- **RQ1:** To what extent are HMRs built using HOMRS better than elementary and randomly selected MRs combinations?
- **RQ2:** How are images transformed by HMRs (built using HOMRS) perceived by humans?
- **RQ3:** To what extent are HMRs built using HOMRS capable of detecting OOD inputs and AE?

Our results show that HMRs generated using HOMRS have a high fault detection capability (*i.e.*, a 95% kill ratio with large effect size); outperforming elementary MRs and their combinations. HOMRS can be used as a simple, lightweight, but effective OOD/AE detector. On our dataset, it detects about 92% of randomly sampled OOD images, as well as 96% of AE. The images transformed using HOMRS-generated HMRs were manually inspected by five independent researchers who confirmed their relevance; therefore providing a validation that HMRs maintain metamorphic properties. Last but not least, HMRs are fast. Their average execution time over 10,000 test images, on a AMD Ryzen 2700x CPU using a single core, is **0.8 ms** per test; which suggests that they can be executed on-line.

This paper makes the following contributions:

- We propose an approach for the generation of an optimized set of HMRs through combination of basic MRs;
- We provide evidences of the effectiveness of HMRs at generating images with a high kill ratio and their ability to detect OOD/AE examples with high accuracy.

The remainder of the paper is organized as follows: **Section 2** provides background on the key concepts used in the approach presented in **Section 3**. **Section 4** reports about the experiments performed to evaluate our proposed approach. **Section 6** discusses the results of our evaluations, while **Section 7** presents the threats to the validity of our study. **Section 8** gives a short overview of related works and **Section 9** concludes the paper.

## 2 BACKGROUND

We applied HOMRS to build HMRs for a DNN used in image classification tasks. This section is intended to provide a brief description of concepts deemed useful to understand our proposed approach.

### 2.1 Deep Neural Networks

DNN are composed of multiple layers of neurons that are tasked with elaborating information from provided inputs. In the basic case of fully-connected DNN, each neuron can be viewed as a function  $f$ , whose inputs are either the input data or the output of other neurons, typically a previous layer. Each neuron has a set of weights  $\mathbf{w} = w_1, w_2, \dots, w_n$  where  $n$  is the number of inputs and a bias  $b$ . If  $\mathbf{x}$  is the neuron input vector, the output of the neuron is computed as  $f(\mathbf{x}) = \sum_{i=0}^n w_i x_i + b$ . Neurons outputs are transformed via a non linear *activation function* “complexifying” the behaviour of the network. Overall, the output of a neuron is computed as  $g(f(\mathbf{x}))$ , where  $g$  is an activation function such as the ReLU function [14]. The input vector is propagated throughout the network until the output where the loss function  $L$  is used to compute the distance to the desired target. From there, a back-propagation algorithm can be used [32] to update the weights. To train DNNs, in traditional settings, the initial dataset is generally split into a train and test set (and possibly a validation set which is used to test for overfitting). The model is trained on the training set and tested on the test set to evaluate its performance on unseen data (generalizability).

### 2.2 Adversarial Examples and Out-Of-Distribution Examples

Given a DNN  $f$  and an image  $\mathbf{x}$  with its ground truth class  $\mathbf{y}$ , an *adversarial example* is defined as an image  $\mathbf{x}'$  such as  $\|\mathbf{x}' - \mathbf{x}\| < \delta \implies f(\mathbf{x}') \neq \mathbf{y}$ , where  $\delta$  is small. It basically include all images which are hard to differentiate from  $\mathbf{x}$  but yield a different prediction through the DNN. We distinguish them from *out-of-distribution* (OOD) examples which are any anomalous example too different from the dataset (“in”) distribution. In our experiments, OOD examples are taken from a different dataset (the DNN wasn’t trained on), whereas adversarial examples are crafted from normal in-distribution examples.

### 2.3 Multi-objective optimization and NSGA-II

Multi-objective optimization aims to tackle problems with conflicting objectives. In our context, we would like to keep the set of HMRs small, but we want it to be very effective in transforming images while also exercising as much as possible the DNN structure. Multi-objective problems are

generally defined as:

$$\begin{aligned} & \min/\max \quad f_m(\mathbf{x}), i = 1, \dots, M \\ & \text{Subject to : } g_j(\mathbf{x}) \geq 0, j = 1, \dots, J \\ & \quad \quad \quad h_k(\mathbf{x}) = 0, k = 1, \dots, K \\ & \quad \quad \quad x_i^{(L)} \leq x_i \leq x_i^{(U)}, i = 1, \dots, n \end{aligned}$$

where  $\mathbf{x} = x_1, \dots, x_n$  represents a solution,  $f_m$  the  $M$  objectives,  $g_j$  and  $h_k$  the constraints of the problem and  $x_i^L$  and  $x_i^U$  the lower and upper boundaries of the  $i$ -th component of  $\mathbf{x}$ .

HOMRS applies NSGA-II (Nondominated Sorting Genetic Algorithm II) to build a Pareto-front, which is the set of non-dominated solutions, where each point represent a solution; hence a HMR. NSGA-II is based on the Genetic Algorithm but applied to a multi-objectives problem. It follows the same principle of *Evaluation*, *Selection*, *Crossover*, and *Mutation* of the base algorithm, but uses: (1) an *elitist* principle, which means that the best solutions of one generation can be carried to the next one, (2) non-dominated solutions through Pareto-front optimization, (3) the *crowded-distance* that maintains population diversity by spreading uniformly the Pareto-front.

## 2.4 Metamorphic Testing & Relations

Let's consider the basic *sine* example from [7]; where  $P$  is a program implementing the *sine* function. The goal is to test  $P$  to see if it matches the mathematical function. Now it might not always be possible to know the exact value of the function for all possible angle values; i.e., the correct value of  $\sin(x)$  for every given  $x$  (the "oracle" problem). However, it is known that  $\sin(x + \pi) = -\sin(x)$ . The relation  $x + \pi$  is what is called a Metamorphic Relation. Leveraging this relation, one could compute for a given *source* test input data  $x$ , a *follow-up* test data  $x + \pi$ , and verify that  $P(x + \pi) = -P(x)$  to test our implementation, without the need for the ground-truth. The identification of these MRs is problem and data dependant. When images are the data and object detection is the problem, MRs should preserve the nature of objects in the images. Simple images based MRs include translation, rotation, shear, scaling, blurring, and contrast.

HMRs can be obtained through "chain" of simple relations [31]. Let  $f_1, \dots, f_n$  be  $n$  simple MRs; a chained relation is defined as the composition of any number of those  $g : f_1 \circ \dots \circ f_n$ . Note that obviously, the functions need to be composable, that is for  $f_j \circ f_i$  we need to have that  $\forall x \in D_i, f_i(x) \in D_j$  where  $D_i, D_j$  are the domain of definition of  $f_i, f_j$ . In our case, since we are dealing with image based transformations, the domain of definition is the same for all transformations. However, contrary to classical chained relations [31], where  $f_i$  are applied to incrementally generate test data and incrementally test the program, we don't aim for the single, known,  $f_i$ , rather for  $g$  the final composition; i.e., intermediate images are not of interest here.

## 3 APPROACH

As shown in Fig. 1, the corner stone of HOMRS is a multi-objective optimization. In the following, we present a detailed description of HOMRS in the context of DNN, image classification, and NSGA-II.

HOMRS takes as input a dataset, a set of MRs relations altogether with relations bounded parameters ranges and a DNN architecture. HOMRS splits the input dataset into, disjoint, train and test sets. The latest, the test set, is actually split into sub-sets, smaller test set partitions. On these sub-sets the meta-heuristic algorithm searches the best sets of HMRs, i.e., the  $g$  chained relations built form the pool of input relations. HOMRS represents an *individual*, a *solution*, as a tree containing one or more HMRs (*genes*). A HMR is a path from the root of the tree to a leaf.

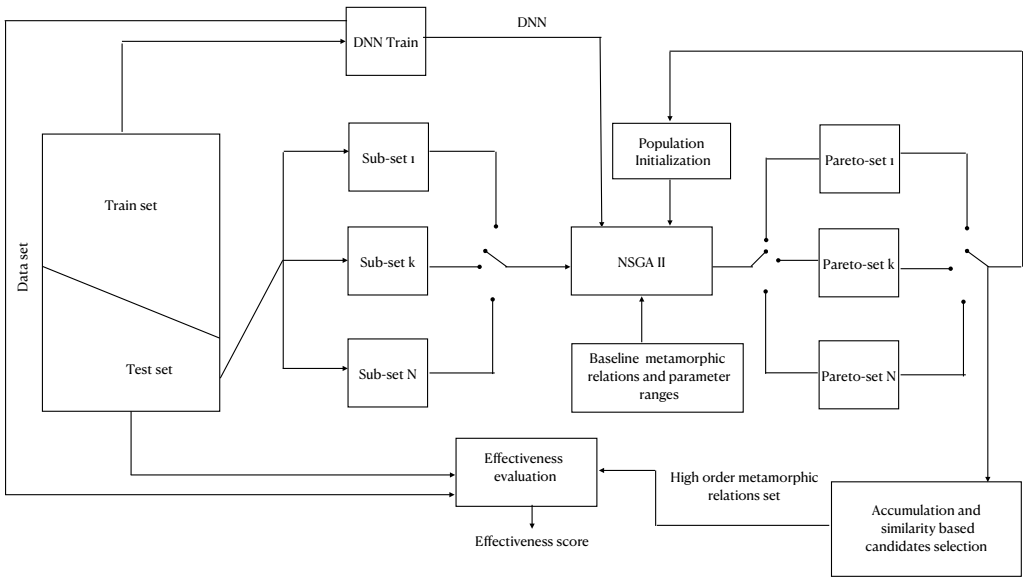


Fig. 1. HOMRS high level view

Note that complexity increases exponentially with the number of HMRs  $K$ , HMRs maximal tree depth  $D$ , and the number of basic types of MRs  $n$ . HOMRS splits the whole test set into smaller sub-sets to reduce off-line computation resources. HOMRS randomly samples  $N$  subsets of size  $S$  smaller than the size of the test set. The assumption is that since we are sampling from the same test set distribution, any relation performing well across the  $N$  subsets should also perform well on the entire test set and thus also on any in-distribution input.

HOMRS runs a multi-objective optimization on each of the sub-sets guided by the fitness functions. Sub-sets data are input to the DNN. The DNN execution is monitored to extract neural patterns. The extracted information and the output of the network guide the search. The search output is a set of Pareto fronts. In order to increase the relevance of the search, HOMRS uses a special kind of elitism. The  $N$  sub-sets are traversed from 1 to  $N$ . At iteration  $i$ , the Pareto front is stored but also used to initialize the population at step  $i + 1$ . The idea is that since we obtain a certain front for a subset (sampled from the test set), it is likely that at least some of those solutions can also be solutions for another subset (or at least be close to the solutions). Finally, once all Pareto fronts are obtained, HOMRS selects the most similar relations sets across the fronts using a similarity matching.

### 3.1 Multi-Objective Fitness Function

To the best of our knowledge there is no clear and formal definition of the notion of MR quality for DNN. Intuitively a good HMR should fulfill the pseudo-oracle task for a DNN. This in turns means that the output of DNN on the original datum, image, and the transformed datum will be different. To assess the quality of HMRs in the context of DNN, we adopt criteria proposed by Segura et al. [33] and adapt concepts of traditional software testing such as code coverage, path coverage, and test case diversity. The first objective function is inspired by code coverage. This idea was previously used to promote traversing DNN neurons [30]. The more code is tested, the more likely defect will be exposed. In DNN terms, the key idea is to check how many neurons were triggered

by the test set compared to the total number of neurons in the DNN. The definition of triggered is generally whether or not the output of the neuron is over a certain threshold (in the case of ReLU activation it is generally 0). Hence, for a test (sub)set  $\mathcal{T}$ , a number of activated neurons  $N_{act}$ , and a total number of neurons  $N_{tot}$ , the coverage is defined as:

$$NCov(\mathcal{T}) = \frac{N_{act}(\mathcal{T})}{N_{tot}}$$

HOMRS uses neuron coverage for two reasons. First, it is the most straight-forward criterion to emulate statement coverage in DNN and, second, it is the criterion used in similar experiment (see Section 4).

The second objective function has the goal to mimic path coverage and test case diversity. We want to maximize the diversity among HMRs while ensuring that different DNN execution paths are exercised. HOMRS adapts the idea of *path coverage* to DNN in the following way. First we define a measure of *neuron similarity*. Let  $t_0$  be a non transformed original test case, and let  $t_k$  with  $k = 1, \dots, K$ , where  $K$  is the number of HMRs to be applied or *follow-up* test cases. In a nutshell, each  $t_k$  is the result of the application to  $t_0$  of a candidate HMR of an individual of the population. Let  $\mathbf{t} = [t_0, t_1, \dots, t_K]$ . We define the neuron similarity of  $\mathbf{t}$ :

$$Nsim(\mathbf{t}) = \frac{1}{N_{tot} \binom{K+1}{2}} \sum_{i \neq j} \sum_j \mathcal{H}(a(t_i), a(t_j))$$

where  $\mathcal{H}$  is the Hamming Distance and  $a(t_i)$  represents the activation trace of the test  $t_i$  through the DNN: it captures the state of activation of each neuron when a test  $t_i$  is passed through the DNN. This measure quantifies how similar are HMRs (and the original test) to each other. We divide it by the number of neurons and combinations in order to obtain a value between 0 and 1. The similarity over the whole test (sub)set  $\mathcal{T}$  is then:

$$NSim(\mathcal{T}) = \frac{1}{|\mathcal{T}|} \sum_i Nsim(\mathbf{t}_i)$$

where  $\mathbf{t}_i$  represents the original/follow-up tests for each test of the test subset inputted to the DNN. This criterion allows for a better spread of the tests path coverage, a better diversity of the paths triggered by each relation. Moreover, it also fills the role of a normal "size" criterion since it penalizes set of relations where the number of relations is too high, as more relations lead to less potential diversity.

The last objective function is inspired by metamorphic testing and measures the error detection effectiveness of the HMRs. HOMRS checks if a test returned a different output through the DNN compared to the output of one of the follow-up tests. The *kill ratio* over the test subset  $\mathcal{T}$  is computed as:

$$KR(\mathcal{T}) = \frac{1}{|\mathcal{T}|} \sum_i \mathcal{B}(\mathbf{t}_i)$$

where,  $\mathcal{B}$  is a boolean function returning 1 if there exists a relation for which the MT fails, 0 otherwise. We average over the whole (sub)set size to have numbers between zero and one. The *kill ratio* measures how many *unique* tests fail: one or more relations returning an error for a given source test will still count as one, as just one relation is needed to detect an error.

Overall, HOMRS uses three objective functions 1) to maximize (neuron) coverage, 2) increase diversity of tests (by minimizing similarity), and 3) maximize the number of unique errors found by HMR sets.

### 3.2 Solution Representation and Genetic Operators

HOMRS individuals are set of chains of MRs, they are rooted trees. A representation of individuals plus the crossover operator are shown in Fig. 2. HOMRS tree root has a variable number, at most  $K$ , of children branching from it. A root-to-leaf path is a HMR.  $K$  is our *budget* number of HMRs in an individual.

Crossover operates on gene paths, swapping HMRs between individuals. Mutation operator is subdivided into three sub-operators. Mutation can either change the value of the parameters (but keep the same relation), nullify the relation (i.e., considering that it is not activated) or reinitialize the relation (new parameters and potentially new relation).

HOMRS restricts the number of relations present in a solution, thus limiting the HMRs execution time. Note that even though we have a maximum budget, we do allow (and encourage) the number of relations used in a solution to be as small as possible while maximizing the three objectives.

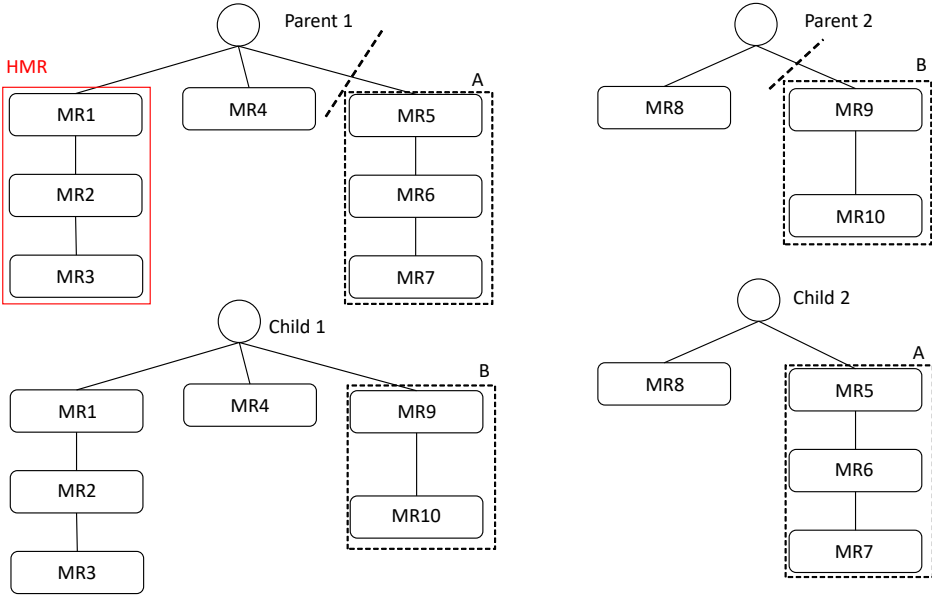


Fig. 2. Single-point crossover operation with examples of individuals. Each individual is composed of multiple HMRs that are the branches of the tree. For instance, the individual represented by “Parent 1” has an HMR [MR1, MR2, MR3] (red), where each MR is a basic metamorphic relation.

### 3.3 Similarity Matching - Selecting the best HMRs

Since each Pareto front is computed on a different sub-set, HOMRS seeks to find the best possible compromise between computed Pareto fronts (sets of sets of HMRs). It starts by finding  $N$  individuals, one for each front, that are mutually the closest in term of transformations and transformation parameters. Let  $Ind_{i,j}$  be the  $j$ -th individual of the pareto front of the subset  $i$ . The goal is thus to find  $N$  individuals  $Ind_{1,j_1}, \dots, Ind_{N,j_N}$  such as:

$$\max_{\mathcal{L}} \sum_{i \neq j} \sum_j \sigma_{\text{Ind}}(Ind_{i,\mathcal{L}_k}, Ind_{j,\mathcal{L}_l})$$

where  $\mathcal{L}$  is the set of combinations of all possible individuals across the fronts and  $\sigma_{\text{Ind}}(Ind_{i,\mathcal{L}_k}, Ind_{j,\mathcal{L}_l})$  is the similarity between the  $k$ -th individual of front  $i$  and the  $l$ -th individual of front  $j$ . That is,

we want to obtain the combination of individual from each front that maximizes their mutual similarity.

The similarity between individual is defined as:

$$\sigma_{\text{Ind}}(\text{Ind}_A, \text{Ind}_B) = \max_C \sum_{p \times q \in C} \sigma_{\text{HMR}}(\text{HMR}_{A,p}, \text{HMR}_{B,q})$$

where  $\sigma_{\text{HMR}}(\text{HMR}_{A,p}, \text{HMR}_{B,q})$  is the similarity between the  $p$ -th HMR of individual A and  $q$ -th HMR of individual B and  $C$  the set of all possible matching between the HMRs of the two individuals. The individual similarity is expressed as the best matching between their respective HMR, *i.e.*, the one giving the maximal similarity. Notice that the order in which HMR appears in the individual is not important.

The similarity between two HMRs is then computed as:

$$\sigma_{\text{HMR}}(\text{HMR}_A, \text{HMR}_B) = \frac{1}{D} \sum_i \sigma_{\text{MR}}(\text{MR}_{A_i}, \text{MR}_{B_i})$$

where  $\sigma_{\text{MR}}(\text{MR}_{A_i}, \text{MR}_{B_i})$  is the similarity between two basic metamorphic relations and  $D$  the maximal HMRs depth. Notice here that, since we have chained relations, order of the basic relations does matter.

Since relations parameters can differ in range, HOMRS first normalizes them between -1 and 1 using the parameters boundaries set for the MRs. Then, HOMRS defines a similarity between two MRs sub-relation as follow:

$$\sigma_{\text{MR}}(\text{MR}_{A_i}, \text{MR}_{B_i}) = \begin{cases} 0, & \text{if } \tau(\text{MR}_{A_i}) \neq \tau(\text{MR}_{B_i}) \\ 1 - \frac{\|\mathbf{x}_{A_i} - \mathbf{x}_{B_i}\|_2}{2\sqrt{n}}, & \text{otherwise.} \end{cases}$$

where  $\tau()$  returns the type of MR (*e.g.*, rotation),  $\text{MR}_{A_i}$  and  $\text{MR}_{B_i}$  are the  $i$ -th relations in the chain of  $\text{HMR}_A$  and  $\text{HMR}_B$ ,  $n$  is the maximum number of parameters a given relation can take in the MRs pool. For instance, the translation transformation for an image takes two parameters.  $\mathbf{x}$  represents the parameters vector. The first condition assigns zero similarity to different MRs, *e.g.*, a translation and a rotation.

The idea of the similarity measures is simply to compare the difference between parameters: the more similar two relations, the closer their parameters. A similarity of zero is obtained when the MRs are of different nature (and both are not null). Otherwise, the similarity is based on the Euclidean distance between the relations parameters divided by the biggest distance that can be obtained. As we have normalized parameters between -1 and 1, the biggest distance is when one relation has parameters that are all equal to 1 and the others are all equal to -1, hence why the  $2\sqrt{n}$ .

Once the  $N$  individuals  $\text{Ind}_{1,j_1}, \dots, \text{Ind}_{N,j_N}$  were obtained, we can obtain a best compromise set of HMRs by taking the average of the parameters of each HMRs of the individuals. This way, we end up making a compromise across the Pareto fronts, and so across the test sub-sets.

Meta-heuristic optimization is stochastic in nature: different runs, with different initial seeds produce different Pareto sets and thus different HMRs. HOMRS runs the off-line computation multiple times with different initial seeds, to ensure HMRs variability. Then it searches HMRs maximizing similarity over the Pareto fronts.

In practice, in our experience, the number of NSGA-II runs does not need to be very high; plus a few independently sampled sub-sets are enough. Also, the budget, *i.e.*, the number of relations chained into an individual, can be kept relatively small: some empirical studies [24] suggest that three to six diverse MRs are enough to reveal a large number of faults. Our experiments confirm these practical considerations.



## 4 EVALUATION

We assess the effectiveness of HOMRS by answering the following Research Questions (RQs):

- RQ1.** To what extent are HMRS built using HOMRS better than elementary and randomly selected MRs combinations?
- RQ2.** How are images transformed by HMRS (built using HOMRS) perceived by humans?
- RQ3.** To what extent are HMRS built using HOMRS capable of detecting OOD inputs and AE?

### 4.1 Procedure

Each RQs required a specific setup detailed in to following.

- To study RQ1, we used a LeNet5 model trained over the MNIST dataset. We apply HOMRS following the block diagram of Fig 1. We train our model on five epochs, using Adam optimizer with default parameters. Achieved test set accuracy was 98.37%. Used MRs are those listed in Table 1; these are MRs previously used in [36]. The range parameters of MRs were selected via trials and error to ensure that images are not modified to the point they would not be similar anymore to the original. We sample five different subsets of the test set (with replacement) with each having a size of  $S = 100$  to have a small enough subset for computation but also representative enough of the set. We fix in all cases a budget of five (so all the individuals are of size five). We set HMRS chains depth to three, again in order not to alter images too much. To quantify the effectiveness of HOMRS against randomly generated relations, we selected individual of size 5 and 20. Size 5 sets are strictly used for comparison purposes, while we use a bigger number of relations relatively to our budget in order to provide evidence that carefully picking the relations is better than increasing their number. Finally we compared HOMRS with a similar tool DeepEvolution; more details are given below.
- To study RQ2, we randomly sample 375 normal images, and further transform them with one HMR so we obtain 375 transformed images, 75 for each transformation. Thus, each set has a size of 750. We repeated the process five times in order to generate five different review sets. We then asked five raters to assign them to a MNIST class, *i.e.*, digit. The sample size was selected to ensure a confidence level of 95 % with a confidence interval of 5%. The goal is to see if the transformations did not change the images to the point they would not be recognizable.
- RQ3 studies HOMRS application to detect AE/OOD, *i.e.*, if HMRS are effective also in detecting nefarious attacks. We proceeded as follows. Firstly, we fine tuned our model by augmenting the training dataset with images generate via HOMRS HMRS in 50% – 50% proportion with normal images. Then we tested the improved model against nefarious attacks. First, we injected 4,000 randomly sampled images from other datasets (FashionMNIST[38], NotMNIST[6], Omniglot[21] and CIFAR-10[20]) *i.e.*, 1,000 images per dataset. We report results out of 30 independent runs. Finally, we also performed FGSM[15] and PGD [25] attacks on 10,000 MNIST test images.

### 4.2 Variable Selection

To answer the research questions we measured different variables. More precisely:

- To study RQ1 we measured the neuron coverage, neuron similarity and kill ratio; we did this for HOMRS as well as the randomly generated HMRS and DeepEvolution.
- To study RQ2, as stated above, we asked five raters to manually classify 750 images; we collected assigned labels and compiled contingency tables.
- To study RQ3 we essentially measured the number of OOD/AE images that HOMRS was able to correctly detect and how many were wrongly detected.

Table 1. Transformations used in our experiments with examples.  $[a, b]^2$  means transformation takes two parameters

Rotation	$[-10, 10]$	Shear	$[-0.1, 0.1]^2$
Translation	$[-2, 2]^2$	Blur	$[0, 1.8]^2$
Scale	$[0.95, 1]^2$	Contrast	$[1, 2]$

### 4.3 Instrumentation and NSGA-II parameters

To carry out the experiment, we implemented a HOMRS prototype in Python. The algorithm is implemented using the framework jMetalPy[4] and TensorFlow 2.1.0. Transformations were generated using OpenCV 4.5.0. Art [29] was used for AE attacks.

NSGA-II parameters were as follows: population size of 50 individuals, a mutation rate of 20 %, a crossover rate of 80 % and 1000 generations. HOMRS has three mutation operators; we set the following mutation operator selection probabilities. Probability of changing value being 0.7; the probability of nullifying the relation being 0.2 and the probability of re-initializing the relation being 0.1. Values were picked empirically to favor exploring neighborhood rather than restarting the exploration.

### 4.4 HOMRS vs DeepEvolution

Similarities can be found between HOMRS and DeepEvolution. Although they are philosophically quite different, it is worth comparing them. DeepEvolution uses evolutionary algorithms to increase neuron coverage by mutating multiple times a small subset of images. HOMRS considers a smaller set of HMRS on a larger set of images. DeepEvolution uses 10 iterations for a population of 10 individuals and a subset of 100 images creating 10,000 potential adversary images.

To make the comparison fair, we did not use the full HOMRS test set but only a subset of it in order to achieve similar number of images. HOMRS HMRS are limited to five relations and thus we use a proportional number of test case images.

Since DeepEvolution uses LeNet which is different from LeNet5 used in RQ1 and RQ3, for the sole purpose of comparing with DeepEvolution, we applied HOMRS to LeNet, all the other parameters being the same as for RQ1.

### 4.5 Data Analysis

We follow recommendations to assess randomized algorithms [2], repeating 30 independent runs in both cases and presenting the average and standard deviation, along with the result of a Wilcoxon test. For RQ2, transformed images were manually validated and we applied Fleiss' Kappa and report its value together with contingency tables.

## 5 RESULTS

**RQ1** deals with HOMRS performance versus a baseline or randomly generated HMR and DeepEvolution. More precisely, we examine the extent to which *HMRS built using HOMRS can outperform elementary and randomly selected MRs combinations*.

### 5.1 HOMRS vs random generation

Comparison of criteria between random and best sets are presented in Table 2 and statistical analysis is presented in Table 3.

Table 2. Comparison of the Effectiveness of HOMRS versus Randomly Sampled Relations Set - Averaged Over 30 Runs. Standard Deviation is Shown in Between Parenthesis.

	NCov	NSim	KR
Test set only	0.9722	-	-
HOMRS (ours)	<b>0.9970</b> (0.0012)	<b>0.7335</b> (0.0113)	<b>0.9518</b> (0.0274)
With random set size 5	0.9903 (0.0045)	0.8422 (0.0311)	0.4194 (0.1882)
With random set size 20	0.9961 (0.0014)	0.8435 (0.0156)	0.6981 (0.1298)

Table 3. Wilcoxon Test p-Values and Cliff’s Delta.  $H_0$ : HOMRS Does not Provide Significant Better Relations Set Compared to Random Method.

Size 5	NCov	NSim	KR
p-value	$1.73 \times 10^{-10}$	$3.02 \times 10^{-11}$	$3.02 \times 10^{-11}$
Cliff’s delta	0.96 (large)	-1 (large)	1 (large)
Size 20	NCov	NSim	KR
p-value	$8.00 \times 10^{-3}$	$3.02 \times 10^{-11}$	$3.69 \times 10^{-11}$
Cliff’s delta	0.398 (medium)	-1 (large)	0.996 (large)

Table 4. Comparison of DeepEvolution Coverage and Number of Adversarial Examples Obtained Against our Method

	NCov	Adv. Examples
DeepEvolution	<b>0.9635</b>	3601
HOMRS (ours)	0.9346	<b>4324</b>

For the test set alone, we only report neuron coverage as other metrics would not have any meaning. It is clear from reported data that HOMRS performs much better than random HMRs generation, regardless of whether they are of length five or twenty. Table 3 confirms that results are statistically significant with a  $p$ -value  $< 0.05$ . Size is not an advantage and when we consider cliff delta 3 the effect size is always large except for neuron coverage (chains of size 20). More importantly, it shows that the budget limit we imposed (sets of five HMRs of maximum length three) for practical use is acceptable as the size of the set will not matter at all for performance. Surprisingly, neuron coverage achieved via bigger sized sets is remarkable while the kill ratios are substantially lower. Thus further strengthening the message that neuron coverage is not a good proxy of how well a DNN is exercised and tested. Note for *Nsim* the criteria is strongly negative as smaller is better for similarity.

Table 5. Averaged Results Among the Participants for the Manual Validation, for Correctly and Wrongly Classified Images, with the Details for Wrongly Classified Images.

Correct	Wrong		
	Modified	Normal	Both
0.9824	0.0053	0.0032	0.0091

Table 6. Confusion Table Representing Correctly/Wrongly Classified Transformed (Transf.)/ Normal (Norm.) Images for each Raters.

	$R_0$	$R_1$	$R_2$	$R_3$	$R_4$
Correct Transf.	366	368	371	368	365
Wrong Transf.	9	7	4	7	10
Correct Norm.	367	367	372	370	370
Wrong Norm.	8	8	3	5	5

## 5.2 HOMRS vs DeepEvolution

DeepEvolution uses multiple evolutionary algorithms that yield different coverage/adversarial example numbers. Remember, that we applied HOMRS to find the best set of HMRS and then we randomly sample  $10,000/n$  images (from the test set) where  $n$  is the number of HMRS in the set. We average the results over three iterations in order to match DeepEvolution procedure. Results are presented in Table 4. We only report the highest score even though results can be achieved by two different algorithms. As we can see, DeepEvolution obtains a better coverage with a score better by 2.9%. This can be explained by DeepEvolution relying on mono-objective that aims to maximize neuron coverage through a lot of mutations. HOMRS uses coverage as one objective, so the best relations set obtained is not necessarily the best possible for this criteria precisely. However, HOMRS generates 700 more adversarial examples, even though the number of adversarial examples generated does not constitute an optimized objective. Note that we handicapped ourselves for comparison purposes; indeed, HOMRS aims to be massively generalizable and the relations obtained could be applied straight to the whole dataset, increasing dramatically the neuron coverage and number of adversarial examples generated. Therefore HOMRS is better in generalization and is more effective on new incoming inputs.

**RQ1** : *Relations obtained with HOMRS are more effective in term of metamorphic properties than randomly selected ones. Moreover, HOMRS manages better performance compare to similar evolutionary algorithm based methods, by considering relations set adapted to the whole test set.*

**RQ2** aims to validate HMRS produced by HOMRS. We examine *how images transformed by HMRS (built using HOMRS) are perceived by humans.*

Indeed, if images are too different and humans cannot correctly classify them one may argue that HOMRS does not generate real HMRS. Notice that, using SSIM score just like in DeepEvolution is not possible here, since we aim to have a versatile method, with the transformations used being whatever is deemed fit in any order, as well as being as generalizable as possible; thus a fixed metric would not help. Although we restricted parameters and depth of chained relations, it is still important to empirically verify the soundness of transformed images. Results of manual labelling are summarized in Tables 5 and 6.

“Modified” and “Normal” columns show the percentage of images of this type that were wrongly assigned while their counterpart did not. “Both” means that both the modified and normal version were wrongly assigned.

As we can see, 98% of each set have been correctly classified by human on average and the remaining ones that have been wrongly classified are not only due to modified images; the biggest part of the misclassification happens on both the normal and transformed image, showing that the transformation did not have an effect on the decision. Moreover, the Fleiss’ Kappa coefficient = **0.972**, which implies an excellent agreement on the results across raters. If it is no surprise that some modified images got wrongly labeled because of the transformation making the comprehension harder, interestingly some normal images got wrongly classified while their transformed version got correctly labeled. Generally it happens when the normal image had some artifacts that could make the decision hard (for instance, between ones and sevens), but the transformation “smoothed” them, allowing for a clearer recognition.

**RQ2** : *Images obtained with HOMRS are still relevant for the neural network as the transformations didn’t modify the images to the point it’s not recognizable for a human.*

**RQ3** aims at quantifying the efficiency of HOMRS at detecting OOD/AE. Specifically, we examine *the extent to which HMRs built using HOMRS are capable of detecting OOD inputs and AE.*

The last research question focuses on MT application to detect OOD and AE. OOD data or hand crafted data are likely more prone to be exposed by MT as image perturbations, especially HMRs, transform OOD images even further and also disrupt input crafted specifically to confuse a model.

However, a model trained only on *clean* MNIST images will detect too many sound HMRs’ produced images as errors, *i.e.*, images transformed via HMRs still representing a valid digit. We thus performed the data augmentation mentioned in Section 4.1 procedure using additional images crafted using train data transformed via our best HMRs set.

The new enhanced model, was then subject again to MT using the HMRs relations on the test set; the obtained kill ratio of 0.0968 means 9.68% of the test set is still perceived as an error. However, the 90% accuracy was deemed sufficient as we drastically decreased the error rate of our sound examples.

### 5.3 OOD detection

For OOD, we use the four datasets detailed at the beginning of the section; images were rescaled to fit images size with MNIST size; they were also (when needed) mapped in gray scale. We further modify Omniglot sampled images to have images with a black background with white symbols to better resemble MNIST digits, *i.e.*, to increase the chances of the network being fooled. Table 7 reports the percentage of images that got detected by at least one of HOMRS HMRs as well as the details for each dataset averaged over 30 experiments, *i.e.*, 30 runs over different sampled sets of OOD using previously mentioned dataset to sample from.

As we can see, HOMRS HMRs detect 92% of the OOD examples. Recall that an example is declared as an error as long as one of the used HMR produces a transformed example yielding a different prediction than the original example through the DNN. Without surprises, CIFAR-10 data are the easiest to detect as they dramatically differ from what the DNN is used to (*i.e.*, MNIST data). Fashion MNIST is the best to evade the detection procedure. However, it is worth underlying that, even though the procedure is pretty simple, HOMRS HMRs managed to reveal at minimum 86 % up to, at best, 97 % of OOD.

Table 7. Details of the Percentage of Killed Examples on all Data and Across the Different Dataset Averaged over 30 Runs. Standard Deviation is Given in between Parenthesis.

	Killed examples
All data	0.9212 (0.0050)
Fashion MNIST	0.8645 (0.0106)
CIFAR-10	0.9728 (0.0051)
NotMnist	0.9560 (0.0043)
Omniglot	0.8919 (0.0110)

Table 8. Results of the second experiments on adversarial examples: FGSM attack detection with  $\epsilon = 0.1$  and  $0.3$ .

$\epsilon$	No MT	TPR	FNR	FPR	TNR	Accuracy
0.1	0.7741	0.9796	0.0204	0.0509	0.9491	0.9560
0.3	0.6626	0.9413	0.0587	0.0465	0.9535	0.9494

Table 9. Results of the second experiments on adversarial examples: PGD attack detection with  $\epsilon = 0.1$  and  $0.3$ .

$\epsilon$	No MT	TPR	FNR	FPR	TNR	Accuracy
0.1	0.6981	0.9874	0.0126	0.0453	0.9547	0.9646
0.3	0.6466	0.9658	0.0342	0.0360	0.9640	0.9646

#### 5.4 Adversarial Attacks detection

We used the 10,000 test images from MNIST and performed FGSM and PGD attacks on those images before injecting them in the DNN. The idea was to assess the usefulness of HOMRS HMRS over those attacks for different value of epsilon. The results are presented in Tables 8 and 9 for FGSM and PGD attacks, respectively. The  $\epsilon$  parameter represents the strength of the perturbation being applied to the image in order to make it adversarial. Presented values are commonly used  $\epsilon$  values.

Tables columns report accuracy with and without Metamorphic Testing (no MT) and the True Positive Rate/True Negative Rate (TPR/TNR), as well as the False Positive Rate/False Negative Rate (FPR/FNR) rates. We consider a case to be positive when an adversarial example is predicted differently than the ground truth and, conversely, negative cases happen when an adversarial example do not change the prediction. True Positive (True Negative) are defined when a Positive case happens but at least one HMR detects it (resp. Negative case happens and no relation raises an error). False Positive/Negative is when the relations behave the opposite of what was expected.

The first thing we notice is that, thanks to HOMRS HMRs best set of relations, the data augmentation manages to enhance the robustness of the model against adversarial examples. This phenomenon is similar to adversarial augmented models that use adversarial examples to train the model. Secondly, using MT, we can see that we managed to defend (even more) against adversarial examples; MT with HMRs achieves a detection rate over 94% with FGSM and PGD attacks.

**RQ3** : *Set of HMRs obtained through HOMRS makes for a simple agnostic proxy for OOD and AE detection, with an accuracy of more than 94%.*

## 6 DISCUSSION

Reported data and figures support the evidence that HOMRS and HMRs outperform simple MRs. We believe HOMRS is general enough as it is based on composition of already known (or discovered) HMRs.

Moreover, HOMRS aims to be versatile as the relations in the pool can be anything the user deems appropriate to test the model. The metamorphic properties of the relations are selected and validated by the user. We provided empirical evidence, in the case of the images transformations we used, that the relations used with the defined parameters range didn't alter them to the point where it wouldn't be useful for the DNN. Yet, there is no strict requirement, as HOMRS do not restrict the type of relations used. Requirements are limited to impose soundness of relations input-output.

One noticeable key advantage of HOMRS HMRs is the possibility to use the small set of HMRs *online*. Indeed, by building a small, but generalized, HMRs set, it is possible to validate DNN decisions in real time. This aspect is very interesting for DNN safety, especially in the context of safety critical components; HOMRS HMRs can be applied to realize a light weight extra layer of security. In particular, we showed that HMRs are a simple but effective tool to tackle the OOD/Adversarial examples. Last but not least, this method has the nice feature of being *agnostic* to the kind of attack/OOD that a system may be subject to: it doesn't require any extra adversarial training or ad-hoc methods for it to work and can be applied universally.

## 7 THREATS TO VALIDITY

We now discuss the threats to validity of our study following common guidelines for empirical studies [40].

*Construct validity threats* concern the relation between theory and observation. In this paper we made a few assumptions about DNN testing when defining quality criteria for MRs. However, each of these assumptions is grounded in a theory that has been proven to be valid in the context of traditional software engineering testing, or in previous studies on DNNs. For example, our assumption that higher neuron coverage contributes to higher fault detection rates is shared by previous DNN testing techniques such as DeepTest[36] and DeepEvolution[3]. The rationale behind this assumption is that the more the decision logic of a DNN is exercised, the higher are the chances of uncovering corner cases leading to the detection of errors.

*Threats to internal validity* concern our selection of datasets, models, frameworks, and analysis method. We mitigated this threat by selecting widespread datasets and models for our study. We also used popular frameworks to reduce the risk of computational errors in our implementations. For optimization, we implemented our algorithm based on NSGA-II which is widely used. We experimented with transformations that are commonly used by DNN studies in the computer vision domain. However, HOMRS can be easily applied to any kind of MRs. During our evaluation of HOMRS, we took a conservative approach; selecting the parameters of transformations that

preserved the relevance of the transformed images. Five experts manually verified the images and confirmed their relevance. We also limited the maximal depth of HMRS to achieve the same goal. In practice, it is left to the user to define the valid range of parameters, to obtain inputs that remain within the input domain range.

*Conclusion validity threats* concern the relation between the treatment and the outcome. We paid attention not to violate the assumptions of our algorithms and models.

*Reliability validity threats* concern the possibility of replicating this study. We have provided all the necessary details required to replicate our study. The datasets and models used are publicly available.

*Threats to external validity* concern the possibility to generalize our results. We have evaluated HOMRS on LeNet5 model using MNIST dataset with commonly available relations. Nevertheless, further validation on different types of relations, and different model architectures are desirable.

## 8 RELATED WORKS

MRs have been used in traditional software programming to test scientific software [19], web services [35] and image software [17] among others[33]. Selection or generation of MRs applied to traditional software was also researched on such as using machine learning and graph-based representation relations to generate new ones [18] which restricts the application to program where such a graph can be used. A concrete form to search for can be used with applications such as relations finding for trigonometry formulas [42], which require to know what to look for. Category-choice framework can also be used [8], but it requires to be able to make category-choice specification for a given problem.

It was then extended to application in Machine Learning and DNN. Basic relations for Machine Learning algorithm were first proposed in [39]. It was then applied to validate both machine learning and DNN such as CNN [11] or LSTM [13] and in all the domains using DNN such as Natural Language Processing [16] or medical imagery [12]. However, not much research has been done on selection and/or generation of MRs targeted to ML algorithm; indeed, methods for traditional software use Control-Flow Graph to derive relations which is not relevant to the case of DNN. We are only aware of a method [34] which uses a reinforcement approach through multi-arms bandit to select MRs for a given problem based on the result of the prediction of the algorithm. Our work differs from their, both on the approach as we are using multi-objective genetic algorithm instead of a learned policy, as well as the selection process as we probe the DNN to get relevant neurons information instead of just exploiting the context information. Moreover, we deal with higher order relations through composition where they only work on elementary ones.

MRs were used as a tool for test generation through search-based methods from a single input; DeepTest[36] uses greedy search based on neurons coverage with driving scene images and DeepXplore[30] similarly uses neurons coverage but through a multi-models joint optimization. DeepEvolution[3] also uses neuron coverage but through evolutionary algorithms. However, where they use MRs for *test cases generation*, we rather focus on MRs *selection* as we try to obtain the best set of relations for a given DNN. Even though the goal is not strictly to generate test cases, we do end up generating some through the application of the relations from our best set over the whole test set. The difference in approach lies in the consideration of application of the relations; where they rather apply multiple MRs which increase coverage on a limited subset of samples, we try to find HMRS that perform equally well on the whole dataset through optimization on a limited amount of subsets, in term of coverage, similarity and errors finding. MRs were also used for adversarial examples detection [27]. They used an embedding to represent images and calculated the difference between transformed and non-transformed images embedding to determine whether it is an adversarial example or not. Their method is a black-box method using embedding and



optimization of threshold for the detection of adversarial examples obtained by PGD attack. We instead focus on white-box approach without optimized threshold for the detection of adversarial examples.

## 9 CONCLUSION

In this paper, we presented HOMRS an approach to select a small set of HMRs in the context of DNN testing. The approach is based on multi-objective optimization with three distinct objectives inspired by traditional software engineering and MT. HOMRS aims at building a small set of HMRs maximizing the neuron coverage and error detection while decreasing the similarity of HRMs generated.

We report evidences showing the effectiveness of the idea through two experiments on the MNIST dataset. In the first experiment, HOMRS was compared to a set of randomly selected chains MRs, *i.e.*, randomly generated HMRs of length 5 and 20. In the second experiment, we contrasted HOMRS with DeepEvolution, a similar DNN MT tool. In both experiments, HOMRS outperformed the competing approach with a measured killing ratio of about 95%, *i.e.*, it effectively detected 95% of DNN miss-classified images against randomized sets and generate more adversarial examples than DeepEvolution while being restricted in term of data.

HOMRS HMRs set is built to be small, and contain HMRs with few chained MRs. This makes HOMRS HMRs suitable for online application. Reported data show the usefulness for test cases generation and error detection, effectively enhancing testing capacity of DNN, but also, the potential straight forward application of the obtained best relations set to OOD/Adversarial Examples detection.

MT is an powerful tool that can help test DNN. We believe HOMRS philosophy can stir the research in a new direction to tackle the MRs selection problem. For future works, we aim to investigate the effectiveness of the method on more complex models and datasets, and improve on our approach, especially the criteria used.

## ACKNOWLEDGMENTS

This work was partially funded by NSERC through the DEEL project

## REFERENCES

- [1] Dario Amodei, Chris Olah, Jacob Steinhardt, Paul Christiano, John Schulman, and Dan Mané. 2016. Concrete Problems in AI Safety. *arXiv preprint arXiv:1606.06565* (2016). <https://arxiv.org/pdf/1606.06565.pdf>
- [2] A. Arcuri and L. Briand. 2011. A practical guide for using statistical tests to assess randomized algorithms in software engineering. In *2011 33rd International Conference on Software Engineering (ICSE)*. 1–10. <https://doi.org/10.1145/1985793.1985795>
- [3] H. Ben Braiek and F. Khomh. 2019. DeepEvolution: A Search-Based Testing Approach for Deep Neural Networks. In *2019 IEEE International Conference on Software Maintenance and Evolution (ICSME)*. 454–458. <https://doi.org/10.1109/ICSME.2019.00078>
- [4] Antonio Benítez-Hidalgo, Antonio J. Nebro, José García-Nieto, Izaskun Oregi, and Javier Del Ser. 2019. jMetalPy: A Python framework for multi-objective optimization with metaheuristics. *Swarm and Evolutionary Computation* 51 (2019), 100598. <https://doi.org/10.1016/j.swevo.2019.100598>
- [5] Battista Biggio and Fabio Roli. 2018. Wild patterns: Ten years after the rise of adversarial machine learning. *Pattern Recognition* 84 (2018), 317–331. <https://doi.org/10.1016/j.patcog.2018.07.023>
- [6] Yaroslav Bulatov. 2011. NotMNIST. <http://yaroslavvb.com/upload/notMNIST/>.
- [7] Tsong Y Chen, Shing C Cheung, and Shiu Ming Yiu. 2020. Metamorphic testing: a new approach for generating next test cases. *arXiv preprint arXiv:2002.12543* (2020).
- [8] Tsong Yueh Chen, Pak-Lok Poon, and Xiaoyuan Xie. 2016. METRIC: METamorphic Relation Identification based on the Category-choice framework. *Journal of Systems and Software* 116 (2016), 177–190. <https://doi.org/10.1016/j.jss.2015.07.037>

- [9] M. Chu, C. Murphy, and G. Kaiser. 2008. Distributed In Vivo Testing of Software Applications. In *2008 1st International Conference on Software Testing, Verification, and Validation*. 509–512. <https://doi.org/10.1109/ICST.2008.13>
- [10] K. Deb, A. Pratap, S. Agarwal, and T. Meyarivan. 2002. A fast and elitist multiobjective genetic algorithm: NSGA-II. *IEEE Transactions on Evolutionary Computation* 6, 2 (2002), 182–197. <https://doi.org/10.1109/4235.996017>
- [11] J. Ding, X. Kang, and X. Hu. 2017. Validating a Deep Learning Framework by Metamorphic Testing. In *2017 IEEE/ACM 2nd International Workshop on Metamorphic Testing (MET)*. 28–34. <https://doi.org/10.1109/MET.2017.2>
- [12] J. Ding, X. Li, and X. Hu. 2019. Testing Scientific Software with Invariant Relations: A Case Study. In *2019 IEEE 19th International Conference on Software Quality, Reliability and Security (QRS)*. 406–417. <https://doi.org/10.1109/QRS.2019.00057>
- [13] Anurag Dwarakanath, Manish Ahuja, Sanjay Podder, Silja Vinu, Arijit Naskar, and Koushik MV. 2019. Metamorphic Testing of a Deep Learning based Forecaster. arXiv:1907.06632 [cs.LG]
- [14] Xavier Glorot, Antoine Bordes, and Yoshua Bengio. 2011. Deep Sparse Rectifier Neural Networks. In *Proceedings of the Fourteenth International Conference on Artificial Intelligence and Statistics (Proceedings of Machine Learning Research, Vol. 15)*, Geoffrey Gordon, David Dunson, and Miroslav Dudík (Eds.). JMLR Workshop and Conference Proceedings, Fort Lauderdale, FL, USA, 315–323. <http://proceedings.mlr.press/v15/glorot11a.html>
- [15] Ian J. Goodfellow, Jonathon Shlens, and Christian Szegedy. 2015. Explaining and Harnessing Adversarial Examples. arXiv:1412.6572 [stat.ML]
- [16] Pinjia He, Clara Meister, and Zhendong Su. 2020. Structure-Invariant Testing for Machine Translation. In *Proceedings of the ACM/IEEE 42nd International Conference on Software Engineering (Seoul, South Korea) (ICSE '20)*. Association for Computing Machinery, New York, NY, USA, 961–973. <https://doi.org/10.1145/3377811.3380339>
- [17] R. Just and F. Schweiggert. 2009. Evaluating Testing Strategies for Imaging Software by Means of Mutation Analysis. In *2009 International Conference on Software Testing, Verification, and Validation Workshops*. 205–209. <https://doi.org/10.1109/ICSTW.2009.20>
- [18] Upulee Kanewala, James M. Bieman, and Asa Ben-Hur. 2016. Predicting Metamorphic Relations for Testing Scientific Software: A Machine Learning Approach Using Graph Kernels. *Softw. Test. Verif. Reliab.* 26, 3 (May 2016), 245–269. <https://doi.org/10.1002/stvr.1594>
- [19] U. Kanewala and T. Yueh Chen. 2019. Metamorphic Testing: A Simple Yet Effective Approach for Testing Scientific Software. *Computing in Science Engineering* 21, 1 (2019), 66–72. <https://doi.org/10.1109/MCSE.2018.2875368>
- [20] Alex Krizhevsky, Vinod Nair, and Geoffrey Hinton. [n.d.]. CIFAR-10 (Canadian Institute for Advanced Research). [n. d.]. <http://www.cs.toronto.edu/~kriz/cifar.html>
- [21] Brenden M. Lake, Ruslan Salakhutdinov, and Joshua B. Tenenbaum. 2015. Human-level concept learning through probabilistic program induction. *Science* 350, 6266 (2015), 1332–1338. <https://doi.org/10.1126/science.aab3050> arXiv:<https://science.sciencemag.org/content/350/6266/1332.full.pdf>
- [22] Y. LeCun, B. Boser, J. S. Denker, D. Henderson, R. E. Howard, W. Hubbard, and L. D. Jackel. 1989. Backpropagation Applied to Handwritten Zip Code Recognition. *Neural Computation* 1, 4 (1989), 541–551. <https://doi.org/10.1162/neco.1989.1.4.541> arXiv:<https://doi.org/10.1162/neco.1989.1.4.541>
- [23] Y. Lecun, L. Bottou, Y. Bengio, and P. Haffner. 1998. Gradient-based learning applied to document recognition. *Proc. IEEE* 86, 11 (1998), 2278–2324. <https://doi.org/10.1109/5.726791>
- [24] H. Liu, F. Kuo, D. Towey, and T. Y. Chen. 2014. How Effectively Does Metamorphic Testing Alleviate the Oracle Problem? *IEEE Transactions on Software Engineering* 40, 1 (2014), 4–22. <https://doi.org/10.1109/TSE.2013.46>
- [25] Aleksander Madry, Aleksandar Makelov, Ludwig Schmidt, Dimitris Tsipras, and Adrian Vladu. 2019. Towards Deep Learning Models Resistant to Adversarial Attacks. arXiv:1706.06083 [stat.ML]
- [26] Rohan Reddy Mekala, Gudjon Einar Magnusson, Adam Porter, Mikael Lindvall, and Madeline Diep. 2019. Metamorphic Detection of Adversarial Examples in Deep Learning Models with Affine Transformations. In *Proceedings of the 4th International Workshop on Metamorphic Testing (Montreal, Quebec, Canada) (MET '19)*. IEEE Press, 55–62. <https://doi.org/10.1109/MET.2019.00016>
- [27] Rohan Reddy Mekala, Adam Porter, and Mikael Lindvall. 2020. Metamorphic Filtering of Black-Box Adversarial Attacks on Multi-Network Face Recognition Models. In *Proceedings of the IEEE/ACM 42nd International Conference on Software Engineering Workshops (Seoul, Republic of Korea) (ICSEW'20)*. Association for Computing Machinery, New York, NY, USA, 410–417. <https://doi.org/10.1145/3387940.3391483>
- [28] Christian Murphy, Kuang Shen, and Gail Kaiser. 2009. Automatic System Testing of Programs without Test Oracles. In *Proceedings of the Eighteenth International Symposium on Software Testing and Analysis (Chicago, IL, USA) (ISSTA '09)*. Association for Computing Machinery, New York, NY, USA, 189–200. <https://doi.org/10.1145/1572272.1572295>
- [29] Maria-Irina Nicolae, Mathieu Sinn, Minh Ngoc Tran, Beat Buesser, Ambrish Rawat, Martin Wistuba, Valentina Zantedeschi, Nathalie Baracaldo, Bryant Chen, Heiko Ludwig, Ian Molloy, and Ben Edwards. 2018. Adversarial Robustness Toolbox v1.2.0. *CoRR* 1807.01069 (2018). <https://arxiv.org/pdf/1807.01069>

- [30] Kexin Pei, Yinzhi Cao, Junfeng Yang, and Suman Jana. 2019. DeepXplore: Automated Whitebox Testing of Deep Learning Systems. *Commun. ACM* 62, 11 (Oct. 2019), 137–145. <https://doi.org/10.1145/3361566>
- [31] Peng Wu. 2005. Iterative metamorphic testing. In *29th Annual International Computer Software and Applications Conference (COMPSAC'05)*, Vol. 2. 19–24 Vol. 2. <https://doi.org/10.1109/COMPSAC.2005.166>
- [32] D. Rumelhart, Geoffrey E. Hinton, and R. J. Williams. 1986. Learning representations by back-propagating errors. *Nature* 323 (1986), 533–536.
- [33] S. Segura, G. Fraser, A. B. Sanchez, and A. Ruiz-Cortés. 2016. A Survey on Metamorphic Testing. *IEEE Transactions on Software Engineering* 42, 9 (2016), 805–824. <https://doi.org/10.1109/TSE.2016.2532875>
- [34] Helge Spieker and Arnaud Gotlieb. 2020. Adaptive metamorphic testing with contextual bandits. *Journal of Systems and Software* 165 (2020), 110574. <https://doi.org/10.1016/j.jss.2020.110574>
- [35] C. Sun, G. Wang, B. Mu, H. Liu, Z. Wang, and T. Y. Chen. 2011. Metamorphic Testing for Web Services: Framework and a Case Study. In *2011 IEEE International Conference on Web Services*. 283–290. <https://doi.org/10.1109/ICWS.2011.65>
- [36] Yuchi Tian, Kexin Pei, Suman Jana, and Baishakhi Ray. 2018. DeepTest: Automated Testing of Deep-Neural-Network-Driven Autonomous Cars. In *Proceedings of the 40th International Conference on Software Engineering (Gothenburg, Sweden) (ICSE '18)*. Association for Computing Machinery, New York, NY, USA, 303–314. <https://doi.org/10.1145/3180155.3180220>
- [37] Elaine J. Weyuker. 1982. On Testing Non-Testable Programs. *Comput. J.* 25, 4 (1982), 465–470. <https://doi.org/10.1093/comjnl/25.4.465>
- [38] Han Xiao, Kashif Rasul, and Roland Vollgraf. 2017. *Fashion-MNIST: a Novel Image Dataset for Benchmarking Machine Learning Algorithms*. arXiv:cs.LG/1708.07747 [cs.LG]
- [39] Xiaoyuan Xie, Joshua W.K. Ho, Christian Murphy, Gail Kaiser, Baowen Xu, and Tsong Yueh Chen. 2011. Testing and validating machine learning classifiers by metamorphic testing. *Journal of Systems and Software* 84, 4 (2011), 544 – 558. <https://doi.org/10.1016/j.jss.2010.11.920> The Ninth International Conference on Quality Software.
- [40] Robert K Yin. 2002. *Applications of Case Study Research Second Edition (Applied Social Research Methods Series Volume 34)*. {Sage Publications, Inc}.
- [41] Bo Zhang, Hongyu Zhang, Junjie Chen, Dan Hao, and Pablo Moscato. 2019. Automatic Discovery and Cleansing of Numerical Metamorphic Relations. In *2019 IEEE International Conference on Software Maintenance and Evolution (ICSME)*. 235–245. <https://doi.org/10.1109/ICSME.2019.00035>
- [42] Jie Zhang, Junjie Chen, Dan Hao, Yingfei Xiong, Bing Xie, Lu Zhang, and Hong Mei. 2014. Search-Based Inference of Polynomial Metamorphic Relations. In *Proceedings of the 29th ACM/IEEE International Conference on Automated Software Engineering (Vasteras, Sweden) (ASE '14)*. Association for Computing Machinery, New York, NY, USA, 701–712. <https://doi.org/10.1145/2642937.2642994>